Hole drift in PDATS

1994 J. Phys.: Condens. Matter 6 2047

(http://iopscience.iop.org/0953-8984/6/10/022)

J. Phys.: Condens. Matter 6 (1994) 2047–2058. Printed in the UK

Hole drift in PDATS

N E Fisher

Department of Aeronautical Engineering, Queen Mary and Westfield College, Mile End Road, London E1 4NS, UK

Received 23 November 1993, in final form 11 January 1994

Abstract. Using a technique entailing localized photo-generation of excess carriers on the (100) face of a PDATS crystal, an asymmetry between the distances holes drift and those of the electrons is found. By modelling the electric fields between surface electrodes, an average distance for the hole drift is estimated, and is deduced to be about 60 μm with lower and upper bounds of 40 and 80 μm respectively. Further experiments suggest that the holes do not undergo any form of recombination but could remain in the crystal for long times. The effect of this in this and other photo-conduction experiments is considered.

1. Introduction

The principal aim of this paper is to describe a simple experimental technique that demonstrates that following the creation of excess charge carriers on the surface of the photo-conductive polymer crystal bis(p-toluene sulphonate) ester of 2,4-hexadiyne-1, 6-diol (PDATS), the generated positive charge remains trapped in the crystal on a time scale of at least seconds and that it is therefore the drift of the negative carriers only that is primarily responsible for the photocurrents observed in many related photo-conduction experiments. This technique is an extension of a time-of-flight experiment already reported by us, and so before describing our current arrangement, we shall briefly review our previous results and the relevant experimental arrangement along with a background of PDATS.

PDATS is easily produced as millimetre-sized single crystals in which the polymer backbone direction is well defined and common to all chains in the sample [1]. Because the chain separation is large (0.7 nm) compared to the repeat unit distance on a chain (0.45 nm) [2], each chain may be considered as an independent quasi-one-dimensional semiconductor. Dark-conductivity measurements along the perpendicular to the chains by Siddiqui and Wilson [3] show an anisotropy of over 1000 reflecting this one-dimensional nature. The interest in PDATS then, is that it offers an insight into quasi-one-dimensional carrier motion.

Fisher and Willock [4–6], using three separate and different time-of-flight techniques (one of which will be described here), find trap-limited time-of-flight signals for electrons only and corresponding featureless decays for the holes. We concluded therefore that the electrons were the dominant current carriers. Furthermore, the drift velocities of the electrons were found to be acoustic (varying between 400 m s^{-1} to 3000 m s^{-1} for applied electric fields of 0.5×10^6 V m^{-1} to about 7.0×10^6 V m^{-1}) with observed trap-limited mobilities of the order of 10^{-4} m^2 s^{-1} V^{-1}. In addition, the time-of-flight profiles were found to become more ill defined (tending towards featureless decays) as the applied fields were reduced or the sample temperature lowered, and this we attributed to increased dispersive carrier propagation due to a lengthening of field-dependent and temperature-dependent trap-release times. We also found that those crystals grown in an oxygen-free environment (to be termed

oxygen-free crystals) exhibited significantly less deep and shallow trap concentrations than those grown in the presence of oxygen, and it is these oxygen-free crystals that are again used in the experiments presented here.

Using uniform illumination techniques in which all the sample is illuminated, these basic conclusions of trap-limited transport down to small distances and low mobilities are in agreement with work of, for example, Moses and Heeger [7] and Blum and Bassler [8] but not that of Donovan and Wilson [9, 10] who, in their experiments, report ultra-high low-field mobilities (20 $m^2\ s^{-1}\ V^{-1}$) and large inter-trap distances (1 mm).

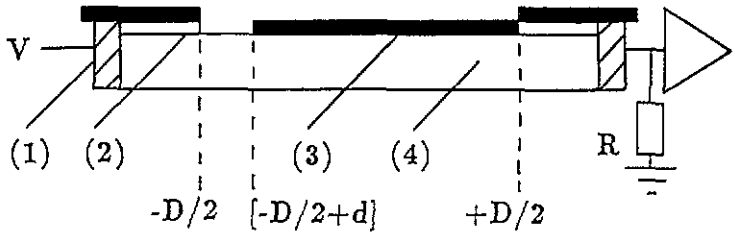

Figure 1. The experimental arrangement for a transit-current experiment on the (100) face of the PDATS crystal: (1) silver paste; (2) evaporated silver electrodes of separation D; (3) opaque optical mask with slit of width d; (4) PDATS crystal. Following an incident laser pulse, carriers are generated at the slit. Depending on the polarity of V, one sign of carrier transverses the sample to induce a transit signal while the other discharges at its nearest electrode.

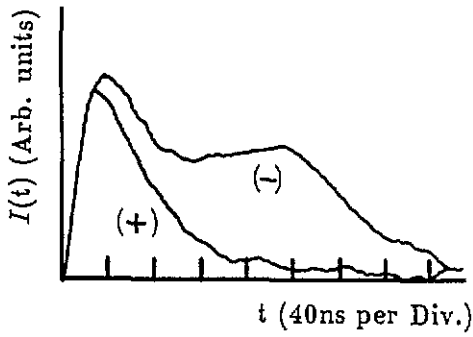

Figure 2. Transit currents obtained with D = 240 μm using an applied V of 700 V: (-) left electrode negative; (+) left electrode positive.

We now summarize our results in figure 1, which shows a time-of-flight arrangement using localized carrier generation on the surface of the PDATS crystal, and figure 2, which shows the typical photo-currents obtained. As stated earlier, no obvious time-of-flight signal is observed for the hole photo-current (obtained when the applied voltage V is made positive) and, as in all our other experiments, we could not ascertain with any degree of certainty whether these generated holes were actually stationary during the experiment, implying therefore that all the photo-currents observed are primarily due to the drift to and discharge of electrons at their nearest electrode, or if the holes were drifting and undergoing such dispersive transport, that any time-of-flight signal becomes featureless [11]. In addition, because the amplifiers used were fast (in order to observe the fast electron signals) and could not therefore be used in the second or even microsecond time regimes, it was not possible to identify any long-time hole time-of-flight signatures, should they exist. In order to try to answer some of these questions we use a variation of the arrangement of figure 1, which is described next.

2. Experimental method and operation

The experimental arrangements are twofold: in the first case, the set-up is that of figure 1 with a fast amplifier and oscilloscope used to observe the transient photo-currents, and in the second case, it is again that of figure 1 but this time with a Keithley 610C Coulombmeter and chart recorder employed in place of the amplifier to measure the total charge induced on the electrode to which it is connected. In both cases, the sample is held under a vacuum of about 10^{-6} Torr during the experiment. To generate carriers in the crystal, two light sources are used: as in previous experiments we employ a 10 ns (FWHM), 3.68 eV laser pulse and in addition to this (using a white light source, transmission filters and a camera shutter), a 1 s exposure of blue light of photon energy about 2.64 eV. In both cases, carriers are generated on the surface of the crystal in a skin depth of about 5 μm. The sample itself on which these experiments are conducted is oxygen free, of total length about 5 mm, width about 1.3 mm and has silver surface electrodes evaporated onto its (100) face with an inter-electrode distance D of about 370 μm. Finally, as in previous experiments, the width d of the slit cut in the optical mask is about 60 μm.

We shall now briefly review the theory behind the observables measured, because, as will become clear, they become fundamental to the analysis and interpretation of forthcoming results.

In a conventional two-electrode photoconductivity experiment, a general result is that the charge dq' induced on the electrodes, due to a sample charge q drifting a distance x, is given by

$$dq' = (q/V)\, dV(x) \tag{1}$$

where V is the potential between the electrodes and $dV(x)$ is the potential change through which the charge drifts. Since $E(x) = -dV(x)/dx$ where $E(x)$ is the electric field between the electrodes, then

$$dq' = -(q/V)E(x)\, dx \tag{2}$$

and

$$dq'/dt = I(t) = -(q/V)E(x)v_d \tag{3}$$

where v_d is the drift velocity of the sample charge. From this we see that equation (2) relates to the observable measured by the Coulombmeter and equation (3) relates to that measured by the amplifier.

3. Results and analysis

3.1. Distance of hole drift

Using the 'second-case' experimental arrangement described earlier, figures 3 and 4 each show the measured charge Q_m induced on the electrodes when V is -300 V and when V is +300 V, for illumination with the blue light and for illumination with the laser light respectively. Two observations are apparent from these data. In figure 4, unlike figure 3, the charge generated tends towards sub-linearity with increased laser intensity and this we take to be due to bimolecular recombination—something that is not observed using the blue light because of its much longer pulse duration and hence its generation of carrier sheets with much lower charge densities. More important, however, is the observation that there is asymmetry between the magnitudes of the Q_m values with respect to the polarity of the

applied voltage (to which we henceforth refer to as $-Q_m$ when V is negative, and $+Q_m$ when V is positive) and which gives here an average ratio, $R_1 = -Q_m/+Q_m$, of about -3.5. We show typical examples of the measured Q_m values in figure 5. Assuming that in both cases equal quantities of charge are initially generated, we see from equation (2) that this asymmetry must stem from a difference in the average distance traversed by the electrons with respect to that traversed by the holes and it is to the determination of an estimation of that distance of hole drift to which we now turn.

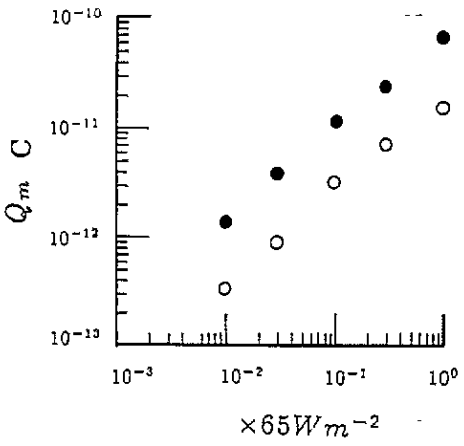

Figure 3. The measured induced charge dependence on blue light intensity using an applied V of 300 V: filled circles, $-Q_m$; open circles, $+Q_m$.

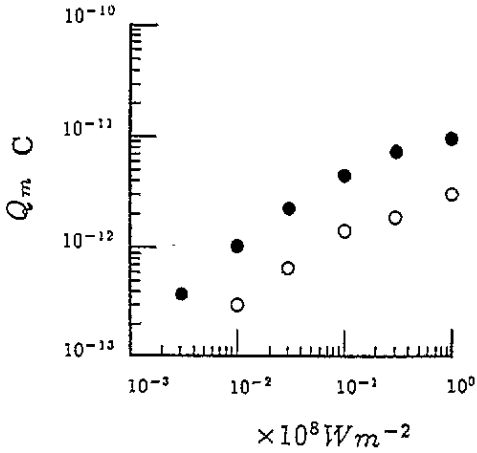

Figure 4. The measured induced charge dependence on laser light intensity using an applied V of 300 V: filled circles, $-Q_m$; open circles $+Q_m$.

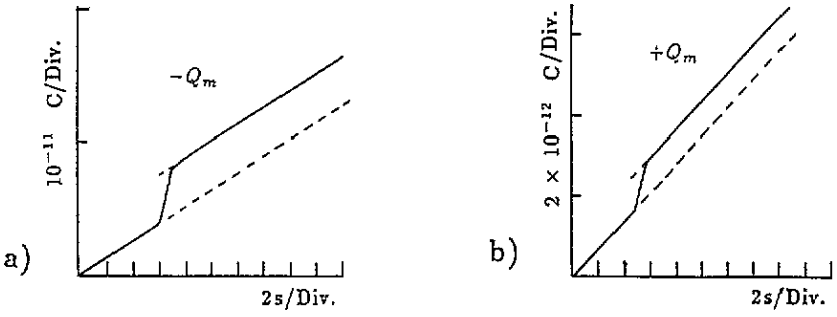

Figure 5. The induced charge (superimposed on the dark current) as measured on a chart recorder in response to a 1 s exposure to blue light of intensity 2 W m^{-2}: (a) applied V is -300 V; (b) applied V is +300 V.

Fisher and Willock [12], using uniform illumination techniques to determine whether Shockley–Read [13] recombination centres existed in oxygen-free PDATS crystals, found approximate linearity between the Q_m values measured on different samples (normalized to the width w of each sample) and their inter-electrode distances (which ranged from 0.24 mm to 9.18 mm). They thus deduced (from equation (2)) that for those charge carriers that are mobile, recombination centres are absent and that on average they can traverse the whole

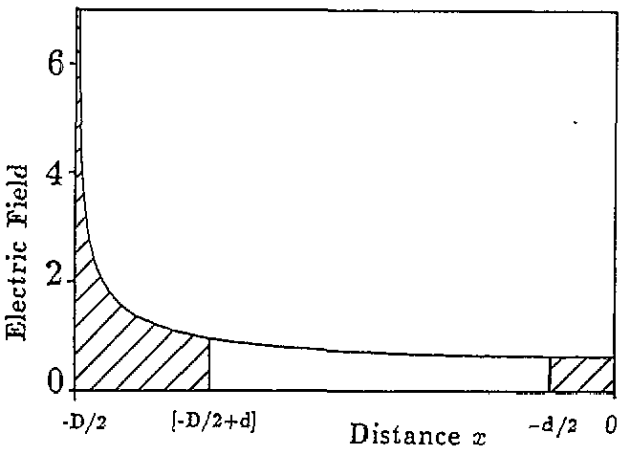

Figure 6. The electric field, normalized to units of its mean field between $-D/2$ and $+D/2$, following equation (5) with $C = 1$. The shaded areas represent the position of a carrier sheet generated near an electrode and half a carrier sheet generated in the middle of the sample. The field becomes infinite at the electrodes.

length of the crystal on a scale of at least millimetres. Based on this conclusion and the time-of-flight techniques discussed earlier, the dominant current carriers are the electrons and so (with reference to figure 1 and equation (2)) we can estimate the average distance traversed by the holes using

$$R_1 = \left(-\int_{(x_0)}^{(D/2)} E(x)\,\mathrm{d}x + \int_{(x_0)}^{(x_1)} E(x)\,\mathrm{d}x\right) \Big/ \left(-\int_{(x_0)}^{(-D/2)} E(x)\,\mathrm{d}x + \int_{(x_0)}^{(x_2)} E(x)\,\mathrm{d}x\right) \quad (4)$$

where the first term in both the numerator and the denominator refers to the contribution to the charge induced on the electrodes due to electron drift and the other two terms refer to that due to hole drift; x_0 is the position of the centre of charge of the initially generated carrier sheet between $-D/2$ and $(-D/2+d)$; x_1 is the final position of the centre of charge of the hole carrier sheets when the applied voltage is negative and x_2 is its final position when the applied voltage is positive.

In order to solve equation (4) we need to know the field distribution $E(x)$ between the surface electrodes. However, because these are at the surface, we cannot use the simple relation $E(x) = V/D$ applicable to parallel-plate geometry and so must now attempt to model the actual internal fields.

Firstly, analytically for infinite surface electrodes the field distribution follows

$$E(x) = (2/\pi)(V/D)\left[C - (2x/D)^2\right]^{-1/2} \quad (5)$$

where C is a constant and in this case equal to unity [14, 15]. If we could determine from experiment the ratio R_2 of the mean field $\langle E\rangle^{\mathrm{e}}$ sampled by a carrier sheet near the electrode with that $\langle E\rangle^{\mathrm{m}}$ sampled by a carrier sheet in the middle of the sample (say) then

$$\langle E(x)\rangle^{\mathrm{e}}/\langle E(x)\rangle^{\mathrm{m}} = R_2 \quad (6)$$

where $\langle E(x)\rangle$ (following equation (5)) can be determined analytically with a varying parameter C to be solved for, which satisfies equation (6). Hence, having solved for C we should then have deduced an electric field distribution that follows the form of the analytic solution, but one that reflects experiment better and also one in which the electric fields do not become infinite at the electrodes.

In order to determine this ratio R_2 we use the 'first-case' experimental arrangement and record the magnitudes of the peak photocurrents (I) following a 10 ns laser pulse when the optical slit is positioned next to one of the electrodes (which gives I^e), when it is positioned in the middle of the sample (which gives I^m) and when it is positioned next to the other electrode (which again gives I^e) for both polarities of V; in each case we find I^e/I^m is about six [16]. Thus, if we now take into account the fact that the field dependence of the charge generated on this particular sample is weakly superlinear with an exponent of 1.2 [16] (in accordance with the superlinear field dependence of one-dimensional carrier pair separation as predicted by for example Blossey [17]) and also the fact that, except at the highest applied fields, the drift velocity of the dominant current carriers is approximately linear with the applied field [4] (a conclusion also reached by others, e.g. [7]) then with reference to equation (3) and figure 6, which shows a plot of the electric field following equation (5) (with $C = 1$) and the position of the carrier sheets with respect to it,

$$\left(\langle E\rangle^e/\langle E\rangle^m\right)^{3.2} = 12 \tag{7}$$

where here $\langle E\rangle^e$ is the mean electric field sampled by the carrier sheets generated between $x = -D/2$ and $(-D/2 + d)$ and $\langle E\rangle^m$ is the mean field sampled by the carrier sheets generated between $-d/2$ and 0. Thus, in this case R_2 is 2.174.

Since $\int E(x)\,dx = [D/2]\sin^{-1}(ax)$ where a is $2/(DC^{1/2})$, then from equation (7)

$$\left[\sin^{-1}(ax)\right]/d\Big|_{(-D/2)}^{(-D/2+d)} = \left[\sin^{-1}(ax)\right]2.174/(d/2)\Big|_{(-d/2)}^{(0)} \tag{8}$$

which gives, by inputting the known parameters, the relation

$$\sin^{-1}\left(1/C^{1/2}\right) - \sin^{-1}\left(\left(1/C^{1/2}\right)25/37\right) = 4.348\,\sin^{-1}\left(\left(1/C^{1/2}\right)6/37\right). \tag{9}$$

Solving numerically we find that $C^{1/2}$ is 1.009 272 914. A plot of the field distribution $E(x)$ following equation (5) with this value of $C^{1/2}$, which thus satisfies the experimentally deduced relation of equation (7), is shown in figure 7.

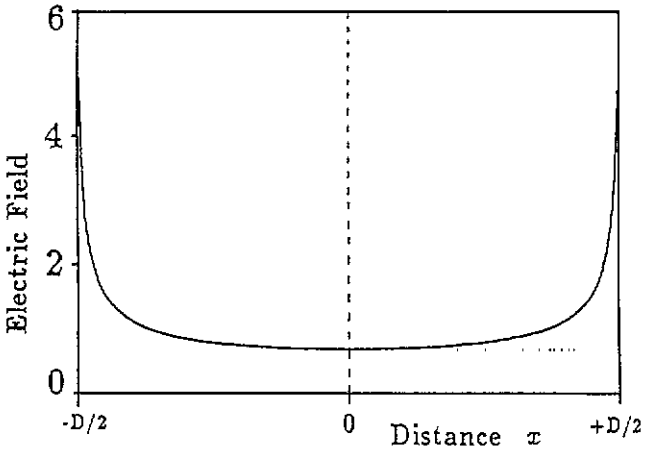

Figure 7. The electric field, normalized to units of its mean field between $-D/2$ and $+D/2$, following equation (5) with $C^{1/2}$ = 1.099 272 914. In this case the field is 5.1 units at the electrodes.

Having approximated the internal electric fields we can now find the centre of change x_0 of a carrier sheet generated near an electrode. (We justify the use of x_0, which is to be used in the following analysis, shortly.) Because the charge $Q(x)$ generated follows the form $[E(x)]^{1.2}$, we can find x_0 by finding the mean charge $\langle Q \rangle$ generated between $x = -D/2+d$ and $x = -D/2$ and then deduce x_0 using $\langle Q \rangle = Q(x_0)$. Solving $\langle Q \rangle$ numerically gives x_0 at $-166(.79)$ μm which is about 18 μm from its nearest electrode. (If we had said that $Q(x)$ simply follows the form $E(x)$, then $\langle Q \rangle$ can be evaluated analytically, which then gives x_0 at $-165(.98)$ μm or about 19 μm from the electrode. For the purposes of estimating hole drift distances these differences are negligible but for completeness we shall use the former value of x_0.)

To solve equation (4) we have to consider two scenarios. In the first case if the holes drift on average a distance less than 18 μm then we define $x_1 = x_h$ and $x_2 = (2x_0 - x_h)$. From equation (4), this gives

$$\left[R_1 + 1\right] \sin^{-1}(aD/2) + R_1 \sin^{-1}(ax_2) - \sin^{-1}(ax_1) = 0 \tag{10}$$

where again $a = 2/(DC^{1/2})$. There is in fact no real solution for x_h that satisfies equation (10) and its substituted values, so we consider the second-case scenario, in which the holes on average can drift a distance greater than 18 μm. Here, x_1 is now equal to $-D/2$ and x_2 is equal to x_h and so from equation (4) we have the relation

$$\sin^{-1}(ax_h) = -\left[2/R_1 + 1\right] \sin^{-1}(aD/2). \tag{11}$$

Solving for x_h, the average position to which the holes drift when the applied voltage is positive, gives the value $-107(.74)$ μm which implies therefore that on average the holes drift no more than 60 μm.

We can also estimate a lower and an upper bound for this hole drift based on two extremes of $E(x)$. In the first case it may be possible that we have underestimated the ratio R_2 of equation (6) because a fraction of the charge generated near the electrode discharges during the duration of the laser pulse which (obviously) does not occur when the charge is generated in the middle of the sample. Hence, I^e may be underestimated with respect to I^m and so therefore is the mean field at the electrode. The limit in this scenario is when C of equation (5) is equal to unity. Following previous steps, x_0 is now at about $-170(.25)$ μm and from equation (11), x_h is now at about $-115(.34)$ μm which implies therefore that here the holes traverse an average distance of about 55 μm. The opposite extreme case occurs if the electric field distribution simply follows V/D. With the centre of charge of the carrier sheets now at their mid-points then from equation (4) (which now is in effect a ratio of distances) the average distance the holes would drift is about 76 μm.

Another possible source of error is d, which was measured to be about 60 μm. A gross under- and overestimate of this value would be if d were actually 40 or 80 μm (say). Then, following previous steps, the centre of charge using the field distribution of figure 7 would be at $-172(.23)$ or $-161(.60)$ μm which implies therefore that the average distance traversed by the holes is about 65 or 54 μm respectively. It is encouraging therefore that such (artificially) large uncertainties do not significantly affect the deduced values of hole drift distance.

A final possible source of error is in determining the ratio R_1, which is deduced from chart recorder data. This can be more difficult to find accurately, as the laser or blue light intensity is reduced for the same applied V, since the dark current can tend to 'swamp' the Q_m on which it is superimposed (see figure 5). Again, a slightly exaggerated under- and overestimate would be if this value were -3 or -4. Using the field distribution of

figure 7, equation (11) gives x_h as at $-85.(95)$ or $-122.(77)$ μm which implies that the average distance traversed by the holes is about 80 or 44 μm respectively.

We also note that if the holes are actually stationary then, based on the electric field distribution of figure 7, equation (10) (with $x_1 = x_2 = x_0$) implies that R_1 would be about -7.68, and if the field distribution simply follows V/D then it would be about -11.33, which are both well above the value observed (including any experimental uncertainty). We thus conclude that the holes do drift a small distance, which is estimated to be on average between 40 and 80 μm and possibly about 60 μm. A final implication is that $-Q_m$ is then a reasonable indication of the actual charge generated.

We now finally attempt to justify the use of x_0 as a reasonable indicator for the average distances carrier sheets drift, as used above. We consider an elemental charge at an initial position X between $-D/2$ and $-D/2+d$, which can drift either to $+D/2$ or $-D/2$ under the action of the electric field $E(x)$ of figure 7. The induced charge q' is then

$$q' \propto \left[\sin^{-1}(ax)\right]Q(X)\Big|_X^{+D/2} \qquad \text{and} \qquad q' \propto \left[\sin^{-1}(ax)\right]Q(X)\Big|_X^{-D/2} \tag{12}$$

respectively where $Q(X)$ is that amount of charge generated at X following the form $[E(x)]^{1.2}$. Figure 8 shows these plots. If we now sum all the induced charges due to all the elemental charges each drifting their own individual distances to, in one case, $+D/2$ and in the other, $-D/2$, and then take their ratio, we would than have modelled the ratio $-Q_m/+Q_m$ for electrons (say) with the holes stationary, which are generated in a slit of width d next to one electrode, without making any assumptions regarding the centre of charges. Numerically calculating this, with as before $-D/2 = -185$ μm and $d = 60$ μm gives, using 600, 6000 and 12 000 elements, the answers -7.655, -7.631 and -7.630 respectively. Such small changes in these answers for large changes in the number of elements suggests that we are fast approaching an analytic answer and it is very encouraging that it is close to the value of $-7.68(4)$ deduced above using the centres of charges. In fact, with the field distribution simply following V/D we find a ratio -11.333, which is the same as that deduced before.

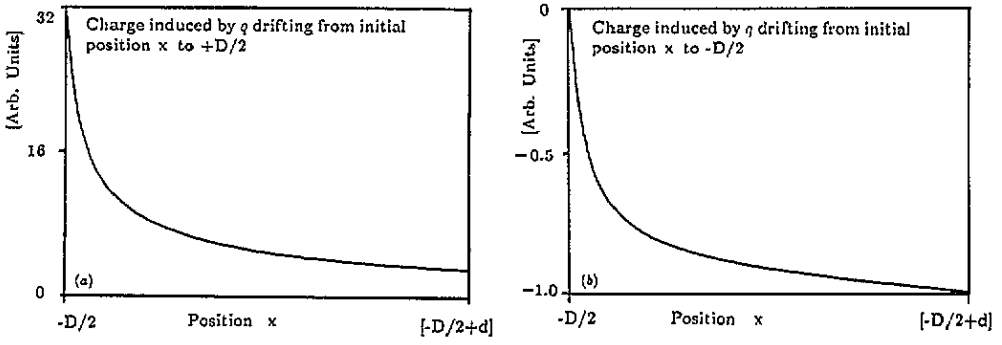

Figure 8. (a) A plot of induced charges due to elemental charges drifting from x to $+D/2$. (b) A plot of induced charges due to elemental charges drifting from x to $-D/2$. In both cases they drift under the action of $E(x)$ of figure 7 with an initial charge distribution following $E(x)^{1.2}$.

3.2. Shockley–Read recombination

It would also be interesting to know whether the holes undergo a Shockley–Read type recombination during drift or whether some (if not all) remain in the crystal (still retaining

their positive charge). The following experiment suggests that it is the latter scenario that holds. Here we use the 'first-case' experimental arrangement of figure 1 and employ two procedures for obtaining results. In the first procedure we apply an electric field to the sample, then shine the blue light onto the slit and, after 1 s pulse with the laser (with the blue light still incident). The peak photo-current ($-I_b$ when V is negative and $+I_b$ when V is positive) and the transition region of the transit current due to the laser pulse are recorded. In the second procedure, the electric field is applied for 1 s before pulsing with the laser and then recording the induced currents. Figure 9 summarizes the behaviour of $+I_b$ and $-I_b$ with blue light intensity.

Before commenting on these results we note an important point: as in our previous experiments, the laser intensity used is low (approximately 10^5 W m^{-2}) so that any space charge effects [18] by the generated carriers themselves in disturbing the applied fields in the crystal are small, i.e. the condition $Q \ll CV$, where Q is the charge generated and C is the capacitance of the system, is satisfied. This is not the case for the 1 s exposure of blue light where from figures 3 and 4, at maximum intensity, the number of carriers generated is about 1000 times greater than that generated by the laser. We would therefore expect some form of space charge effect if sufficient charge (particularly of one sign only) remains trapped in the crystal.

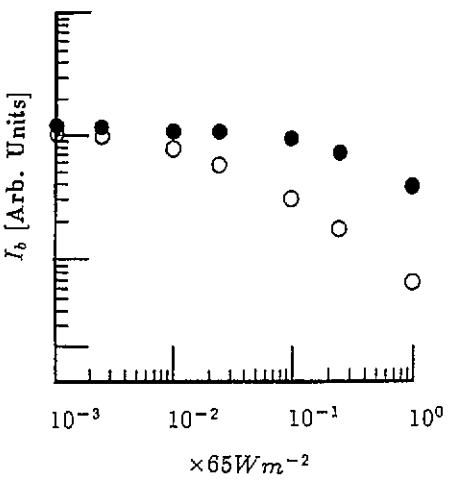

Figure 9. The peak photo-current dependence, induced by a laser pulse following a 1 s exposure to blue light, with blue light intensity: filled circles, applied V = −300 V; open circles, V = +300 V.

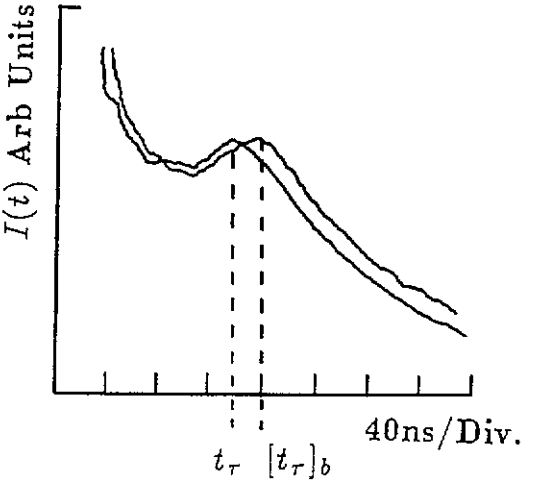

Figure 10. Transit times t_r and $[t_r]_b$ of transition regions obtained with a laser pulse, and a laser pulse following a 1 s exposure to blue light, respectively.

Returning to figure 9, we note that both $-I_b$ and $+I_b$ decrease with an asymmetry that increases with increasing blue light. Two possibilities may explain this. Firstly, if a significant fraction of the positive charges generated by the blue light remain trapped around the region of the slit (and in the case of a positive V, also beyond), then those negative carriers generated by the laser pulse will be prone to recombination with them, hence leading to an overall reduction in I. In addition to this, because the degree of recombination will be polarity dependent (i.e. there will be less recombination if V is negative because there is a loss of some positive charge generated by the blue light due to discharge by the time the laser pulse is incident) then this will also lead to asymmetry of I. Secondly, we must also consider the space charge affect: if sufficient holes generated by the blue light remain

trapped around the region of the slit without undergoing any form of recombination, then their positive charge will reduce the internal electric fields around that region when V is positive, and enhance the electric fields when V is negative, which again will lead to an asymmetry in I.

So, following on from this, a fundamental condition from electrostatics is that $\int E(x)\,dx$ is constant. Thus if, for instance, the field is increased around the region of the slit (in this case when V is negative) then the overall field around the rest of the sample will be reduced. Figure 10 shows the transition regions of two typical transit currents both obtained using the same negative applied V, but in one case the first procedure is used with the highest intensity blue light, and in the other the second. We note from this that the transit time obtained in the first case (with the additional blue light) is longer than that obtained in the second, and because the drift velocity of the carriers is field dependent, this suggests that the leading edge of the electron carrier sheet samples an overall reduced field across most of the sample in accordance with the described space charge effect. As expected, with the intensity of the blue light reduced, the transit time gradually lessens to its second-case value.

To summarize then, albeit qualitatively, the reduction of the magnitudes of both $-I_b$ and $+I_b$ and their asymmetries using large intensities of blue light, are due to a combination of recombination with the positive charge generated by the blue light, the degree of which is polarity dependent, and their consequent space charge effects, which again are polarity dependent. A consequence of an enhanced field, due to the positive charge around the region of the slit when V is negative, is an overall reduction of field around the rest of the sample and this is evidenced by observations of small but observable changes in transit times. We thus conclude that for this to occur at least some of the positive charge does not undergo Shockley–Read recombination during the time scale of the experiment.

These results and conclusions could be said to have implications for those of section 3.1 since it could be argued that the asymmetries of $-Q_m$ and $+Q_m$ are due to a convolution of distances traversed and polarity-dependent space charge and recombination effects. However with reference to this, we note a few points: the data of figure 3, because of its approximate linearity and approximate constant asymmetry even at the highest blue-light intensities suggests that any perturbations due to space charge effects in measuring Q_m values are relatively small. In addition to this, and probably as expected, recombination effects are also small here, because even at the blue light's highest intensity the rate of carrier generation is still 10^5 times less than that with the laser pulse, i.e. if there is a build up of positive charge due to the blue light around the region of the slit and electrons are continually moving away from or discharging at their nearest electrode, then those generated by a subsequent laser pulse are much more prone to recombination with that positive charge than those continually generated by the blue light, because of their much higher charge density. Hence, we might expect polarity-dependent recombination effects using laser and blue light but not blue light alone. In the case of figure 4 recombination effects do occur but because carrier generation occurs within 10 ns, the amount of bimolecular recombination will be approximately polarity independent because in such a short time scale the degree of hole discharge is relatively small, i.e. independent of the sign of V; the generated electrons drift through (approximately) equal quantities of holes and so (both) are subject to about the same degree of recombination. Hence, the asymmetry of figure 4 is again predominantly due to distance drift.

These arguments admittedly entail a little 'hand-waving', but probably the most important point to note is that in using low blue-light intensities, figure 9 shows that $-I_b$ and $+I_b$ are almost the same and yet the asymmetry of figure 3 at about those same intensities still persists (the same is true for the laser light). Since I is dependent on the amount

of charge generated and its drift velocity, both of which are field dependent, this lack of significant asymmetry implies that polarity-dependent space charge and initial recombination effects are small which once again suggests that the asymmetries of figure 3 (especially) at low light intensities are in the main due to distance drift.

We finally note as a point of interest that we performed these same experiments using below-band-gap red (1.69 eV) and infra-red (1.44 eV) light [16]. Here, photo-generation is assigned to the ionization of defects [19] with a skin depth that is considerably larger than that using the blue or laser light and which consequently leads to a charge creation throughout the bulk of the sample. The ratio in this case of $-Q_m/+Q_m$ is about -1.7. However, at present it is not possible to deduce too much from this because we have to consider not only those carriers that are drifting through the surface electric fields, but also those that drift through the smaller electric fields in the bulk of the sample and which could therefore allow carriers to drift under the surface electrodes. However, if the charge measured on the electrodes is dominated by carriers drifting on or near the sample surface (by virtue of the larger electric fields there), this might suggest that the holes traverse a greater distance slightly deeper in the sample than those generated on the (100) face presumably because of the absence of surface trapping states. However, it should be stressed that this is just speculation. A better experimental arrangement would be a sandwich-type electrode configuration on the (011) face with, as before, an optical mask on the (100) face. Then, it should be possible to probe carrier transport on the surface and in the bulk of the sample without the problems discussed above.

We also noted that the peak photo-currents induced by the laser pulse (with the additional red and infra-red light shone onto the sample beforehand) again showed an asymmetry with respect to the polarity of V (along with a change in transit time), but this time, for a negative applied V, the magnitudes of the peak photo-currents showed a small but gradual increase with increased red and infra-red light intensity. We speculate that this may be because the positive charge generated by this light increases the electric field around the region of the slit (as before) but because a larger fraction of this charge lies deeper in the sample than that generated by the laser pulse, recombination between this charge and the electrons generated by the laser is less dominant.

4. Conclusions

We hope that we have shown that, at the very least, there is asymmetry between the distances the holes drift and those of the electrons. By attempting to model the surface electric fields, we estimate that the distance of this hole drift is on average around 60 μm. In addition, the asymmetries of the peak photo-currents along with the changes in transit times, suggest a recombination effect and a space charge effect due to positive charge, which in turn implies that some (if not all) of the holes do not undergo Shockley–Read recombination on a time scale at least as long as the transit-current experiment.

Unfortunately, from these data we cannot ascertain whether the holes predominantly become trapped during drift, or if there is some extreme asymmetry between the electrons' and holes' pre-trapping mobility, or a combination of both. However, the fact that even on a time scale of many seconds these holes appear not to traverse the whole sample length, as suggested by figure 5, implies that deep trapping may be the limiting factor.

These results may also have implications for other photo-conduction experiments. In all our experiments on PDATS, using time-of-flight or uniform-illumination techniques, we found that during repetitive laser excitation, the induced photo-currents diminished in size with the applied fields on and reverse photo-currents were observed with the applied fields

off. This phenomenon has been well observed and reported by Blum and Bassler [8] and they attribute it to space charge accumulation within the crystal reducing the internal applied fields. Based on the above conclusions it now seems likely that the holes are responsible for this, not only by causing space charge effects but possibly providing centres for negative carriers generated by subsequent laser shots to recombine with. Hence, as were those of Blum and Bassler, our experiments were conducted under single-shot conditions in which the sample was irradiated by the laser with the sample shorted between laser shots, until no reverse current was observed.

We finally note that by using much shorter laser-pulse durations along with narrower optical mask slits, it should be possible to determine in a more direct way the distance of hole drift by reducing the inter-electrode distance D between surface electrodes until the magnitudes of $-Q_m$ and $+Q_m$ become equal. Then, any assumptions regarding the internal electric fields need not be considered.

Acknowledgments

My thanks go to Professor D N Batchelder (Leeds University) for informative discussions about this work and to Dr B J E Smith for supplying excellent quality PDATS crystals. The experiments presented here were conducted at the Department of Physics, Queen Mary and Westfield College, London. This work has been supported by the SERC (UK).

References

[1] Wegner G 1969 *Z. Naturf.* b **24** 824
[2] Pope M and Swenberg C E 1982 *Electronic Processes in Organic Crystals (Monographs on Physics and Chemistry of Materials 39)* (Oxford: Oxford Science Publications)
[3] Siddiqui A S and Wilson E G 1979 *J. Phys.: Condens. Matter* **12** 4237
[4] Fisher N E and Willock D J 1992 *J. Phys.: Condens. Matter* **4** 2517
[5] Fisher N E 1992 *J. Phys.: Condens. Matter* 4 2543
[6] Fisher N E 1993 *J. Phys.: Condens. Matter* **5** 85
[7] Moses D and Heeger A J 1989 *J. Phys. C: Solid State Phys.* **1** 7395
[8] Blum T and Bassler H 1988 *J. Chem. Phys.* **123** 431
[9] Donovan K J and Wilson E G 1981 *Phil. Mag.* B **44** 9
[10] Donovan K J and Wilson E G 1985 *J. Phys. C: Solid State Phys.* **18** L51
[11] Scher H and Montroll E W 1975 *Phys. Rev.* B **12** 2455
[12] Fisher N E and Willock D J 1992 *J. Phys.: Condens. Matter* 4 2533
[13] Shockley W and Read P R 1952 *Phys. Rev.* **87** 835
[14] Smythe W R 1969 *Static and Dynamic Electricity* 3rd edn (New York: McGraw-Hill)
[15] Donovan K J, Fisher N E and Wilson E G 1989 *Synth. Met.* **28** D557
[16] Fisher N E 1990 *PhD Thesis* University of London
[17] Blossey F D 1974 *Phys. Rev.* B **9** 5183
[18] Many A, Weisz S Z and Simhony M 1962 *Phys. Rev.* **126** 1989
[19] Chance R R and Baughman R H 1976 *J. Chem. Phys.* **64** 3889